Effect of excess superthermal hot electrons on finite amplitude ion-acoustic solitons and supersolitons in a magnetized auroral plasma

O. R. Rufai,[1,a)] R. Bharuthram,[2,b)] S. V. Singh,[3,c)] and G. S. Lakhina[3,d)]
[1]*Council for Scientific and Industrial Research, Pretoria, South Africa*
[2]*University of the Western Cape, Bellville, South Africa*
[3]*Indian Institute of Geomagnetism, New Panvel (W), Navi, Mumbai-410218, India*

The effect of excess superthermal electrons is investigated on finite amplitude nonlinear ion-acoustic waves in a magnetized auroral plasma. The plasma model consists of a cold ion fluid, Boltzmann distribution of cool electrons, and kappa distributed hot electron species. The model predicts the evolution of negative potential solitons and supersolitons at subsonic Mach numbers region, whereas, in the case of Cairn's nonthermal distribution model for the hot electron species studied earlier, they can exist both in the subsonic and supersonic Mach number regimes. For the dayside auroral parameters, the model generates the super-acoustic electric field amplitude, speed, width, and pulse duration of about 18 mV/m, 25.4 km/s, 663 m, and 26 ms, respectively, which is in the range of the Viking spacecraft measurements. © 2015 AIP Publishing LLC.
[http://dx.doi.org/10.1063/1.4933000]

I. INTRODUCTION

In the laboratory, space, and astrophysics plasmas, several investigations have shown that the particle velocity distributions are not always at Maxwellian equilibrium.[1–9] The particles typically deviated because of having high energy tails attributed to several different acceleration mechanisms.[10,11] These phenomena have been well-modeled using different velocity distributions, such as Lorentzian κ-distribution,[1] Tsallis q-nonextensive distribution[12] and Cairn's nonthermal distribution.[7] In general, Lorentzian κ-distribution has been widely used to analyze and interpret the satellite observations, particularly in the solar wind,[13] the Earth's plasma sheet,[14] Jupiter's magnetosphere,[15] and Saturn's magnetosphere,[3,16] due to the spectral index κ characteristics of Maxwellian-like at lower velocities and power-law form at higher speeds.

Motivated by the spacecraft observations in the auroral region,[17–20] nonlinear electrostatic structures with two-temperature electron have been widely studied.[21–29,31,32] Using Poisson equation, Saini and Kourakis[33] investigated the existence of arbitrary amplitude ion-acoustic solitary waves in an unmagnetized three-component plasma consisting of cold ions, electron beam, and excess superthermal hot electrons. Baluku et al.[30] explored the characteristics of dust ion-acoustic solitons in a dusty plasma with kappa-distributed electrons, using both the reductive perturbation method and the Sagdeev pseudo-potential technique, for the dusty plasma model composed of cold dust particles, adiabatic fluid ions, and superthermal hot electrons. El-Tantawy and Moslem[34] presented the existence conditions for the large amplitude ion-acoustic solitary waves and double layers in an unmagnetized superthermal plasma consisting of

warm positive ions and κ-distribution of hot electrons and positrons. Jung and Hong[35] derived the Korteweg-de Vries (KdV) equation as a function of the spectral index κ and investigated the excess superthermal hot electron effects on the propagation of the ion-acoustic solitary waves in generalized Lorentzian electron-ion plasmas. Singh et al.[36] established a two-component plasma model consisting of adiabatic ion fluid and superthermal hot electrons to study the effect of ion temperature on finite amplitude nonlinear low frequency electrostatic structures in a magnetized auroral plasma. In dusty particles, Alam et al.[37] derived the Burger equation to explore the effect of bi-kappa distributed electrons on dust-ion-acoustic shock waves in unmagnetized superthermal plasmas composed of inertial ions, kappa distributed electrons with two distinct temperatures, and negatively charged immobile dust grains.

Recently, the generation of electrostatic supersoliton structures in the auroral plasma has been the latest development and an interesting topic in space and astrophysics plasmas.[38,42–45] Several plasma models have been explored to show the existence of supersoliton structures in multi-component plasmas, for example, for a plasma model composed of cold positive and negative ions and nonthermal hot electrons studied by Verheest et al.[46] Verheest et al.[47] studied the characteristics of ion-acoustic supersolitons in an unmagnetized plasma consisting of a Boltzmann or kappa velocity distributions model for both cold and hot electron species and cold ions fluid. In a later paper, Verheest et al.[48] described the behaviors of electrostatic supersolitons in dusty plasmas with stationary negative dust, cold fluid protons, and nonthermal electrons. For the first time, Rufai et al.[49] reported the existence of electrostatic supersolitons in magnetized three-component nonthermal plasma using Viking satellite data. Recently, Rufai[50] studied the evolution of nonlinear low frequency electrostatic soliton and supersoliton structures in a magnetized two-ion nonthermal plasma.

a)E-mail: rrufai@csir.co.za
b)E-mail: rbharuthram@uwc.ac.za
c)E-mail: satyavir@iigs.iigm.res.in
d)E-mail: lakhina@iigs.iigm.res.in

In this paper, the effect of an excess superthermal hot electron population is investigated on finite amplitude low frequency electrostatic structures in a magnetized auroral plasma. The plasma model is composed of cold ions fluid, Boltzmann cool electrons, and kappa velocity distribution for the excess superthermal hot electrons. This is an extension of the earlier work of Sultana *et al.*[51] by including Maxwellian cool electrons as a second electron species. In Section II, the governing model is formulated and the characteristics of the localized nonlinear structures using the Sagdeev pseudo-potential technique are presented. Numerical results are discussed in Section III. The conclusions are presented in Section IV.

II. LOW FREQUENCY WAVE MODEL

Obliquely propagating low frequency waves are considered in a three-component, homogeneous, collisionless, and magnetized auroral plasma consisting of cold ion fluid (temperature T_i is neglected), Boltzmann cool electrons (N_c, T_c), and superthermal hot electron (N_h, T_h) having kappa-distribution. The auroral plasma is believed to be embedded in a uniform external magnetic field $\mathbf{B}_0 = B_0 \hat{z}$, where $\hat{z}$ is the unit vector along the z-axis and the nonlinear ion-acoustic waves are propagating in the (x, z) plane obliquely to the magnetic field. The dynamics of the cold ions is governed by the following set of nonlinear fluid equations, namely, the continuity and momentum equations:

$$\frac{\partial N_i}{\partial t} + \nabla(N_i \mathbf{V_i}) = 0, \tag{1}$$

$$\left(\frac{\partial}{\partial t} + \mathbf{V_i} \cdot \nabla\right)\mathbf{V_i} = -\frac{e\nabla\phi}{m_i} + e\frac{\mathbf{V_i} \times \mathbf{B}_o}{m_i c}, \tag{2}$$

where N_i and $\mathbf{V_i}$ are the ions number density and the fluid velocity, respectively, m_i is the ion mass, e is the magnitude of the electron charge, c is the speed of light in vacuum, t is time, and ϕ is the electrostatic potential.

The cool electron density is described by Boltzmann distribution[31,32]

$$N_c = N_{c0} \exp\left(\frac{e\phi}{T_c}\right), \tag{3}$$

while a kappa-distribution function (κ) for hot superthermal electrons[36,52] is adopted

$$N_h = N_{h0}\left[1 - \frac{e\phi}{\left(\kappa - \frac{3}{2}\right)T_h}\right]^{-\kappa+1/2}, \tag{4}$$

where N_{c0}, N_{h0} are the equilibrium densities of the cool and hot electrons, respectively, and κ is the spectral index determining the deviation from thermal equilibrium. The Maxwell-Boltzmann equilibrium in Eq. (3) can be recovered in the limit $\kappa \to \infty$; that is, for the very large values of κ, the superthermal energy distribution function tends to be a Maxwellian distribution.

Normalizing requires appropriate scaling quantities. The densities are normalized with respect to the total ion

equilibrium density $N_{i0} = N_{c0} + N_{h0} = N_0$, velocities by the effective ion-acoustic speed $c_s = (T_{eff}/m_i)^{1/2}$, distance by effective ion Larmor radius, $\rho_i = c_s/\Omega$, and time by the inverse of ion gyro-frequency Ω^{-1}, where $\Omega = eB_0/m_i c$ and potential ϕ by T_{eff}/e. Here, $\tau = T_c/T_h$ is the cool to hot electron temperature ratio, $f = N_{c0}/N_0$ is the cool electron to total electron density ratio, $T_{eff} = T_c/(f + (1-f)\tau)$ is an effective electron temperature $\alpha_c = T_{eff}/T_c$, $\alpha_h = T_{eff}/T_h$, and $\psi = e\phi/T_{eff}$.

The above set of Eqs. (1)–(4) can be presented in normalized form

$$\frac{\partial n_i}{\partial t} + \frac{\partial(n_i v_x)}{\partial x} + \frac{\partial(n_i v_z)}{\partial z} = 0, \tag{5}$$

$$\frac{\partial v_x}{\partial t} + \left(v_x \frac{\partial}{\partial x} + v_z \frac{\partial}{\partial z}\right)v_x = -\frac{\partial\psi}{\partial x} + v_y, \tag{6}$$

$$\frac{\partial v_y}{\partial t} + \left(v_x \frac{\partial}{\partial x} + v_z \frac{\partial}{\partial z}\right)v_y = -v_x, \tag{7}$$

$$\frac{\partial v_z}{\partial t} + \left(v_x \frac{\partial}{\partial x} + v_z \frac{\partial}{\partial z}\right)v_z = -\frac{\partial\psi}{\partial z}, \tag{8}$$

and

$$n_c = f \exp(\alpha_c \psi), \tag{9}$$

$$n_h = (1-f)\left(1 - \frac{\alpha_h \psi}{\kappa - \frac{3}{2}}\right)^{-\kappa+1/2}. \tag{10}$$

It requires defining the quasi-neutrality condition at equilibrium for a low frequency domain, namely

$$n_i = n_c + n_h = fe^{\alpha_c \psi} + (1-f)\left(1 - \frac{\alpha_h \psi}{\kappa - \frac{3}{2}}\right)^{-\kappa+1/2}. \tag{11}$$

The linear dispersion relation for the obliquely propagating low frequency electrostatic waves in a magnetized plasma with Boltzmann cool electrons and superthermal hot electron species and fluid ions can be obtained by solving the continuity and momentuum equations. We assume perturbations to varying as $e^{i(k_x + k_z - \omega t)}$; $k_x = k \sin\theta$ and $k_z = k \cos\theta$, i.e., the wave vector $\mathbf{k}$ makes an angle θ with the magnetic field $\mathbf{B}_0$, and $\frac{\partial}{\partial t} \to -i\omega$, $\frac{\partial}{\partial x} \to ik_x$, $\frac{\partial}{\partial z} \to ik_z$. Then, from Equations (5)–(11), we obtain a linear dispersion relation (unnormalized) given by

$$\omega^2 = c_s^2 k^2 \left(\frac{2\kappa - 3}{(2\kappa - 1) - 2f\alpha_c}\right)\left[\frac{1 - \frac{\Omega^2}{\omega^2}\cos^2\theta}{\left(1 - \frac{\Omega^2}{\omega^2}\right)}\right]. \tag{12}$$

The above equation gives a dispersion relation for obliquely propagating ion-cyclotron and ion-acoustic waves in a magnetized plasma. For low frequency domain ($\omega \ll \Omega \cos\theta$), Equation (12) becomes

$$\frac{\omega}{k} \approx c_s \cos\theta\left(\frac{2\kappa - 3}{(2\kappa - 1) - 2f\alpha_c}\right)^{1/2}. \tag{13}$$

The above equation describes the obliquely propagating ion-acoustic waves in a magnetized plasma. The properties of the linear low frequency waves are displayed in Figure 1 for different values of κ. It is observed that effect of κ is marginal on the frequency of the ion-acoustic waves. This dispersion relation (13) displayed the frequency of the fast mode only since our plasma model contains a single ion species. It is well-known that if plasma contains N numbers of ion species, then the wave frequency is of N modes.[39–41]

In order to examine the nonlinear propagation of arbitrary amplitude ion-acoustic waves, we solve the coupled equations (5)–(11), using the trasformation $\xi = (\alpha x + \gamma z - Mt)/M$, where $M = V/c_s$ is the Mach number (V is the wave speed), $\alpha = \sin\theta$, $\gamma = \cos\theta$; θ is the angle between the direction of wave propagation and the magnetic field. Then, applying appropriate boundary conditions for solitary wave structures (namely, $n_i \rightarrow 1$, $\psi \rightarrow 0$, and $d\psi/d\xi \rightarrow 0$ at $\xi \rightarrow \pm\infty$), and eliminating v_x, v_y, and v_z, we obtain the following:

$$\frac{d}{d\xi}\left(\frac{dP(\psi)}{d\xi}\right) = M^2(n_i - 1) - \gamma^2 n_i H(\psi), \qquad (14)$$

where

$$\frac{dP(\psi)}{d\xi} = \left(1 - \frac{M^2 n_i'}{n_i^3}\right)\frac{d\psi}{d\xi}, \qquad (15)$$

$$H(\psi) = \frac{f}{\alpha_c}(e^{\alpha_c\psi} - 1) + \frac{1-f}{\alpha_h}\left[\left(1 - \frac{\alpha_h\psi}{\kappa - \frac{3}{2}}\right)^{-\kappa+3/2} - 1\right], \qquad (16)$$

and

$$n_i' = \alpha_c f e^{\alpha_c\psi} + \alpha_h(1-f)\left[\left(1 - \frac{\alpha_h\psi}{\kappa - \frac{3}{2}}\right)^{-\kappa-1/2}\left(\frac{\kappa - \frac{1}{2}}{\kappa - \frac{3}{2}}\right)\right]. \qquad (17)$$

Eq. (15) can be reduced to an energy integral
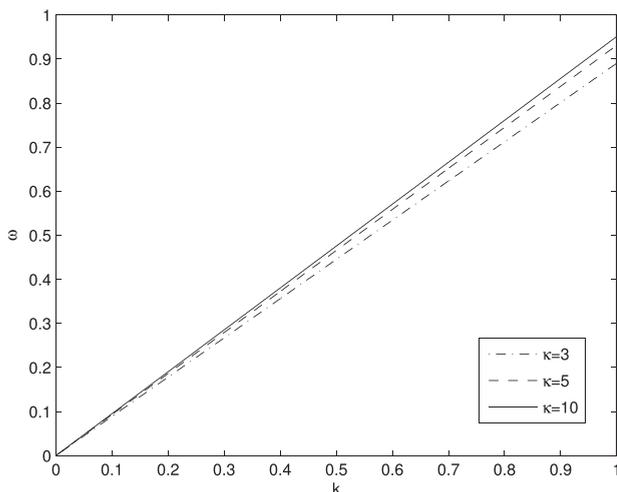
FIG. 1. Dispersion relation: ω against k for $\tau = 0.04$, $\theta = 15$, $f = 0.1$.

$$\frac{1}{2}\left(\frac{d\psi}{d\xi}\right)^2 + V(\psi, M) = 0, \qquad (18)$$

where $V(\psi, M)$ is the Sagdeev potential given by

$$V(\psi, M) = \frac{A(\psi, M) + B(\psi, M)}{\left(1 - \frac{M^2 n_i'}{n_i^3}\right)^2} \qquad (19)$$

where

$$A(\psi, M) = -\frac{M^4(1 - n_i)^2}{2n_i^2} - M^2(1 - \gamma^2)\psi + M^2 H(\psi), \qquad (20)$$

$$B(\psi, M) = -\frac{\gamma^2 H^2(\psi)}{2} - \frac{M^2\gamma^2 H(\psi)}{n_i}. \qquad (21)$$

At $\kappa \rightarrow \infty$, corresponding with the Boltzmann hot electrons limit, the Sagdeev potential $V(\psi, M)$ reduces to Eq. (19) of Rufai *et al.*[31] Then, to examine the evolution of nonlinear low frequency soliton and supersoliton structures, the Sagdeev potential $V(\psi, M)$ must satisfy the following conditions: $V(\psi, M) = 0$, $dV(\psi, M)/d(\psi) = 0$, $d^2V(\psi, M)/d(\psi)^2 < 0$ at $\psi = 0$; $V(\psi, M) = 0$ at $\psi = \psi_m$, and $V(\psi, M) < 0$ for $0 < |\psi| < |\psi_m|$, where ψ_m is the maximum amplitude of the solitons. It must be noted that the additional requirement for a double layer (dl) solution is $dV(\psi, M)/d\psi = 0$ at $\psi = \psi_m$. Then, the supersoliton solution exists when there is an accessible root of the Sagdeev potential beyond the double layer (dl), that is, $V(\psi, M) = 0$ for $\psi > \psi_{dl}$.

The analysis of the second derivative of the Sagdeev potential $V(\psi, M)$, which has to be negative at the origin, namely, $d^2V(\psi, M)/d(\psi)^2 < 0$ at $\psi = 0$, leads to

$$\left.\frac{d^2V(\psi, M)}{d\psi^2}\right|_{\psi=0} = \frac{M^2 - M_0^2}{M^2 - M_1^2} < 0, \qquad (22)$$

where the critical Mach number is

$$M_0 = \gamma\left(\frac{\kappa - \frac{3}{2}}{\left(\kappa - \frac{1}{2}\right) - f\alpha_c}\right)^{1/2} \qquad (23)$$

It must be pointed out here that the critical Mach number, M_0, given by Eq. (23) becomes identical to the root given by Eq. (13) when written in non-dimensional units. Further, for $\kappa \rightarrow \infty$, Equation (23) reduces to a critical Mach number for ion-acoustic mode in two-Maxwellian plasmas.[31] The upper Mach number limit is given by

$$M_1 = \left(\frac{\kappa - \frac{3}{2}}{\left(\kappa - \frac{1}{2}\right) - f\alpha_c}\right)^{1/2}, \qquad (24)$$

since $f\alpha_c + (1 - f)\alpha_h = 1$. For $\gamma = \cos\theta \leq 1$, further analysis of Eq. (22) shows that with $M_1 \geq M_0$, the inequality (22) is satisfied when $M_0 < M < M_1$. Thus, we obtain a condition,

$$\gamma \sqrt{\left(\dfrac{\kappa-\dfrac{3}{2}}{\left(\kappa-\dfrac{1}{2}\right)-f\alpha_c}\right)} < M < \sqrt{\left(\dfrac{\kappa-\dfrac{3}{2}}{\left(\kappa-\dfrac{1}{2}\right)-f\alpha_c}\right)},$$

$$(25)$$

which provides the allowed values of Mach number M of finite amplitude ion-acoustic waves for fixed values of an angle of propagation θ ($\cos\theta = \gamma$), electron density f, superthermal hot electron κ, cool electron temperature α_c, and hot electron temperature α_h. It is important to mention that for the case of $f = 0$, the ion-acoustic waves condition given by Eq. (25) above reduces to Eq. (30) of a magnetized two-component plasma composed of kappa distributed electrons and an inertial ion fluid as reported by Sultana *et al.*[51] On the other hand, condition (25) reduces to the existence condition of the magnetized plasma model consisting of cold ion fluid and Boltzmann distributed electrons studied by Choi *et al.*[53] at $f \to 1$. In the case of Boltzmann distributed hot electron species ($\kappa \to \infty$), the existence condition given by Eq. (25) goes back to Eq. (24) of a magnetized cold ion plasma with two distinct groups of Boltzmann electrons derived by Rufai *et al.*[31]

III. NUMERICAL RESULTS

Figure 2 shows the Mach number ranges (for $\gamma = \cos\theta \neq 1$) that support the existence of finite amplitude nonlinear low frequency electrostatic solitons and supersolitons in auroral plasma. The curves in (a) show the variation of M against κ for $\tau = 0.04$, $f = 0.1$, and $\theta = 15°$, while the graph plotted in (b) shows the variation of M against f for $\kappa = 3$ and 5, for the fixed parameters $\theta = 15°$ and $\tau = 0.04$. The numerical computation values corresponding to the critical and upper Mach number, (M_0 and M_1) obtained from Equations (23) and (24) above. From the chosen parameters, it is important to point out that the ion-acoustic soliton and supersoliton solutions can exist only in the subsonic Mach number regime ($M < 1$). Whereas, in the case of nonthermal electron,[49] the nonlinear solutions were obtained both in the subsonic ($M < 1$) and supersonic Mach numbers regime ($M > 1$).

In Figure 3, the curve shows the variation of the Sagdeev potential $V(\psi, M)$ with the normalized electrostatic potential ψ for different values of the Mach number M. Other fixed parameters are: cool electron number density, $f = 0.1$; angle of propagation, $\theta = 15°$; cool to hot electron temperature ratio, $\tau = 0.04$; and the spectral index, $\kappa = 5$. The negative potential ion-acoustic soliton amplitude ψ increases with increasing Mach number M. As shown in Figure 3, the critical Mach number, $M_0 = 0.93$, and soliton solutions are not found beyond $M > 0.962$. In contrast, for the case of nonthermal electron,[49] the soliton structures are found to be possible for subsonic and supersonic Mach numbers.

Figure 4 shows the normalized electrostatic potential ψ against ξ, which has been obtained through numerical integation of Eq. (19) for the parameters $\tau = 0.04$, $f = 0.1$, $\theta = 15°$, and $M = 0.95$ for different values of κ (superthermal electrons). It clearly shows that as the spectral index κ increases, the soliton amplitude, as well as its width, decreases.
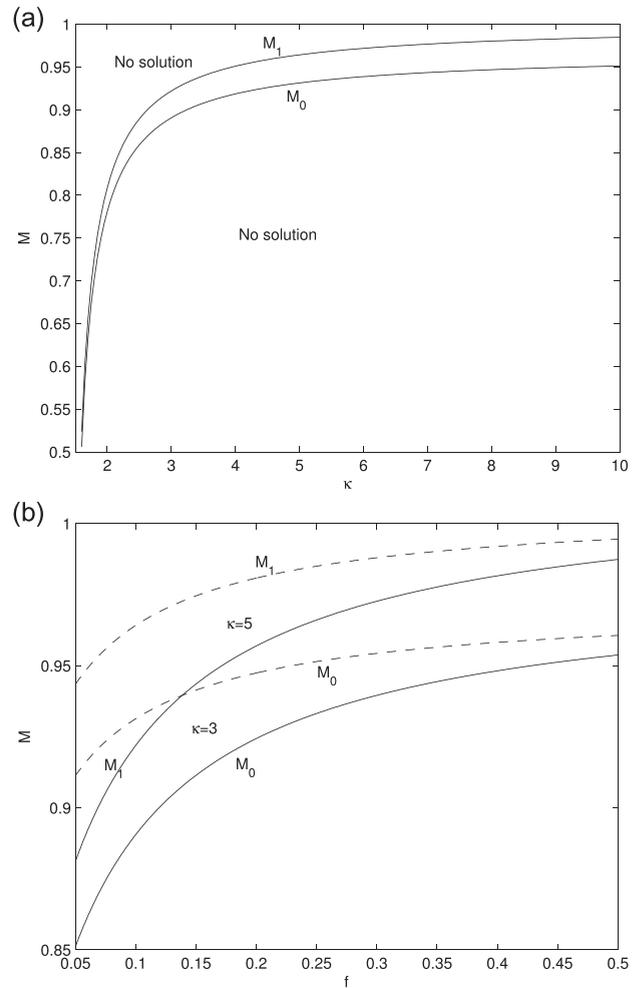
FIG. 2. Variation of critical Mach number, M_0, and upper Mach number, M_1, of nonlinear ion-acoustic structures (a) with superthermal hot electron contribution κ for $\tau = 0.04$, $f = 0.1$, and $\theta = 15°$, (b) with electron density ratio f for $\theta = 15°$ and $\tau = 0.04$.

Figure 5 shows the variation of Sagdeev potential $V(\psi, M)$ with real electrostatic potential ψ for different values for cool electron number density ratio f and for Mach number $M = 0.95$ and other parameters of Figure 3. Further
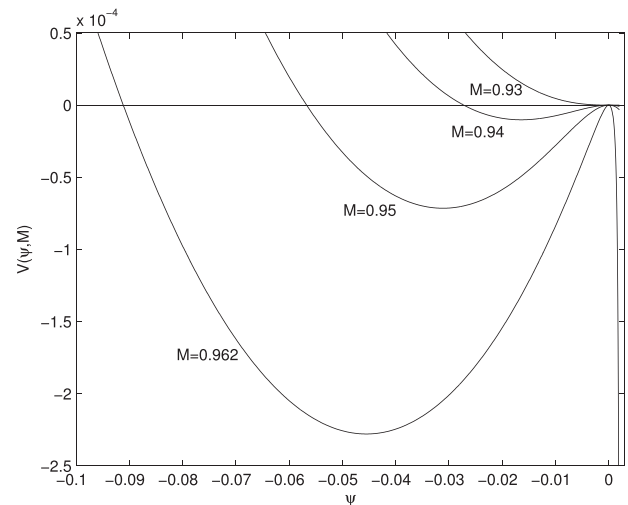
FIG. 3. Sagdeev potential, $V(\psi, M)$, vs. normalized electrostatic potential ψ, for $\tau = 0.04$, $f = 0.1$, $\kappa = 5$, and $\theta = 15°$.
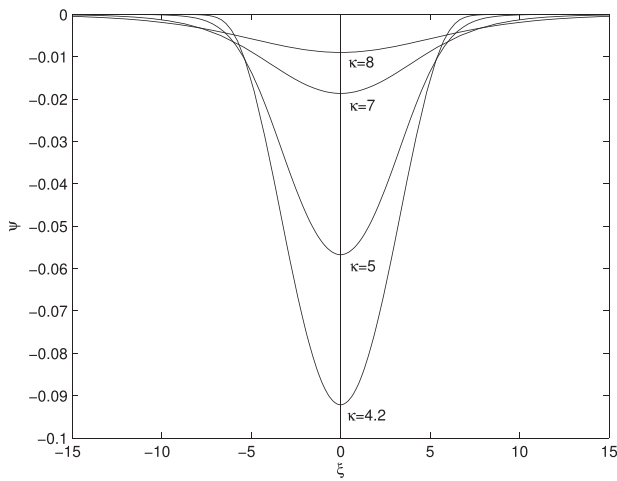
FIG. 4. Normalized electrostatic potential ψ vs. ξ, for $\tau = 0.04$, $f = 0.1$, $\theta = 15°$, and $M = 0.95$.
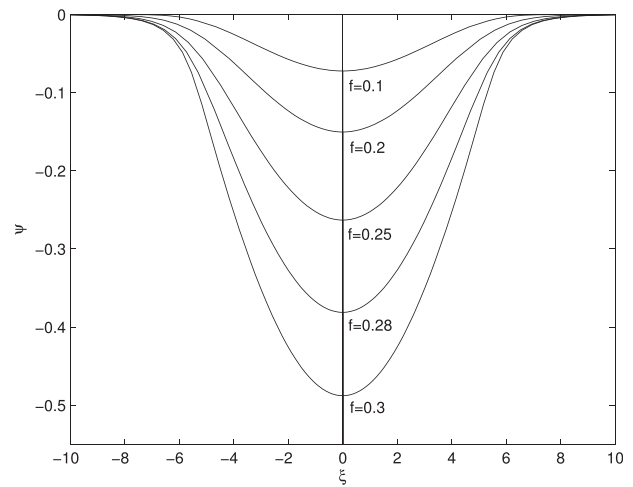
FIG. 6. Normalized electrostatic potential ψ vs. ξ, for $\tau = 0.04$, $M = 0.98$, $\kappa = 10$, and $\theta = 15°$.

numerical computations show that the soliton structures are not possible beyond $f > 0.22$. It is interesting to note that as the cool electron density ratio f increases, the ion-acoustic solitary wave amplitude decreases.

In contrast, for the spectral index $\kappa > 5$, the soliton characteristics change, such that the amplitude and width of nonlinear ion-acoustic soliton increases with increase in f as shown in Figure 6. The fixed plasma parameters are, $\kappa = 10$, $\tau = 0.04$, $\theta = 15°$, and $M = 0.98$. This may be attributed to the fact that as the spectral index κ increases, the hot electrons density distribution function gets more energetic and move towards Boltzmann equilibrium. It shows that the lower values of the spectral index κ represent the velocity distributions with massive superthermal components.[47,51]

The curves plotted in Figure 7 show that the ion-acoustic soliton amplitude increases with the increase in the cool to hot electron temperature ratio τ. The chosen parameters are, Mach number $M = 0.90$, the spectral index $\kappa = 3$, cool electron density $f = 0.1$ and angle of propagation $\theta = 15°$, for the variation of Sagdeev potential $V(\psi, M)$ vs. potential ψ. It is interesting to note that a supersoliton structure appears at

$\tau = 0.0528390102$. For $\tau > 0.0528390102$, there is no supersoliton solutions. The corresponding electrostatic potential profiles of the soliton and supersoliton structures are plotted in Figure 8.

Figure 9 displays the variation of Sagdeev potential $V(\psi, M)$ versus the real potential ψ for a different angle of propagation θ. Other fixed parameters are, $f = 0.1$, $\tau = 0.04$, $\kappa = 10$, and $M = 0.98$. The curves show that as the angle of propagation θ increases (the wave obliqueness $\gamma = \cos\theta$ decreases), the ion-acoustic wave amplitude increases. Interestingly, we note that at $\theta = 34.5023°$, a supersoliton structure appears. Figure 10 shows the corresponding solitons and supersoliton electrostatic potential profiles. It must be pointed out that for the case of nonthermal electron,[49] the supersoliton solution appears at higher values of angle of propagation, $\theta = 39.7302°$ for the same set of plasma parameters. For fixed value of angle of propagation, $\theta = 34.8°$ and other parameters of Figure 9. The Sagdeev potential $V(\psi, M)$ profiles plotted in Figure 11 show that a supersoliton solution is accessible for the Mach number $M = 0.976487$. For $M = 0.99$, no soliton/supersoliton solutions can be found.
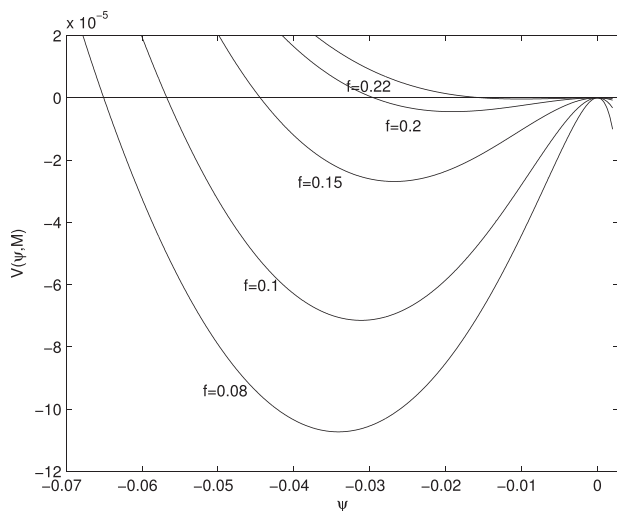
FIG. 5. Sagdeev potential, $V(\psi, M)$, vs. normalized electrostatic potential, ψ, for $\tau = 0.04$, $M = 0.95$, $\kappa = 5$, and $\theta = 15°$.
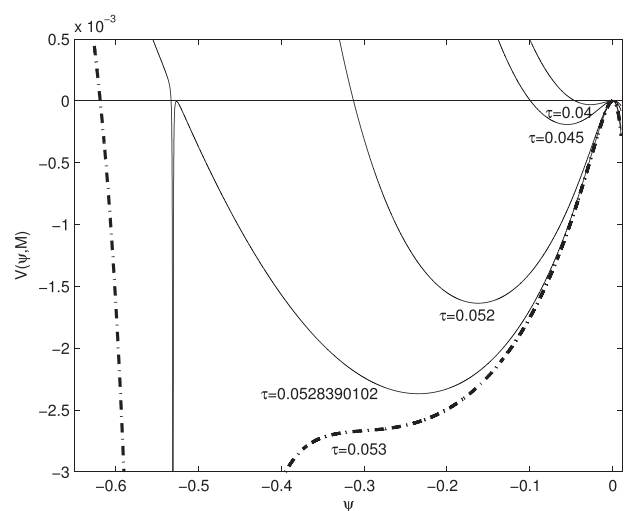
FIG. 7. Sagdeev potential, $V(\psi, M)$, vs normalized electrostatic potential, ψ, for $f = 0.1$, $M = 0.90$, $\kappa = 3$, and $\theta = 15°$.
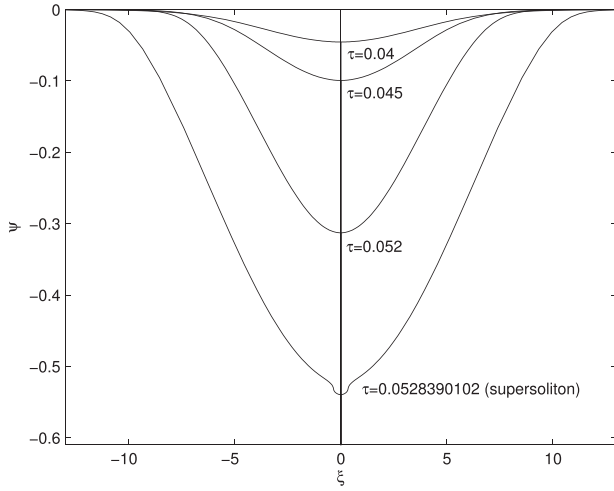
FIG. 8. Normalized electrostatic potential ψ vs ξ, for figure 6 parameters.
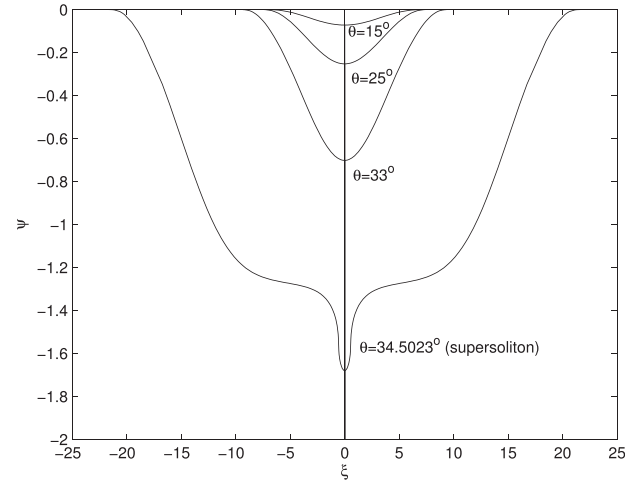
FIG. 10. Normalized electrostatic potential ψ vs. ξ, for Figure 8 parameters.

Table I shows the unnormalized values of the soliton velocity V, electric field E, soliton width W, and pulse duration $\tau^* = W/V$ for various values of spectral index κ, and the Mach number range M, respectively. Using the dayside auroral region parameters,[26] $n_c = 0.2 \, \mathrm{cm}^{-3}$, $n_h = 1.8 \, \mathrm{cm}^{-3}$ $T_c = 1 \, \mathrm{eV}$, $T_h = 26 \, \mathrm{eV}$, gives $T_{eff} \approx 7 \, \mathrm{eV}$. It is seen from Table I that for increasing κ, the critical Mach number M_o, the soliton velocity, and electric field amplitude tend to increase, but with the soliton width and pulse duration decrease. In addition, at the upper Mach number range M_1, only the soliton velocity increases with M_1 and κ, but the maximum electric field, width and pulse duration decrease.

IV. CONCLUSION

In this paper, a detailed investigation was presented of nonlinear propagation of finite amplitude ion-acoustic solitons and supersolitons in a magnetized auroral plasma of cold ions fluid, Boltzmann distributed electron, and excess superthermal hot electron with a kappa velocity distribution. The negative potential low frequency structures are found to exist only in the subsonic Mach numbers regime ($M < 1$).

Whereas, in the absence of Boltzmann electrons, the nonlinear electrostatic structures in two-component plasma have the upper limit at 1.[51] Furthermore, for the case of the Cairns nonthermal distribution model for the hot electron species studied by Rufai *et al.*,[49] the ion-acoustic soliton and supersoliton structures can exist in both subsonic and supersonic Mach numbers regime. The inclusion of the second Boltzmann electrons allowed the existence of the negative potential soliton and supersoliton structures. In the wave obliqueness region, the nonlinear structure appears at the maximum angle of propagation, $\theta = 34.5023°$, which is much lower than in the case of the two Boltzmann distribution electrons model[31] and Boltzmann and nonthermal distributions model,[49] due to the presence of the excess superthermal electrons.

The Viking spacecraft missions in the auroral region of the Earth's magnetosphere have reported[26] the observations of nonlinear low frequency electrostatic fluctuations as follows: electric field amplitude of less than $100 \, \mathrm{mV/m}$, width of about $100 \, \mathrm{m}$, pulse duration of about $20 \, \mathrm{ms}$ and velocities in the range of about 10–$50 \, \mathrm{km/s}$. The present study is
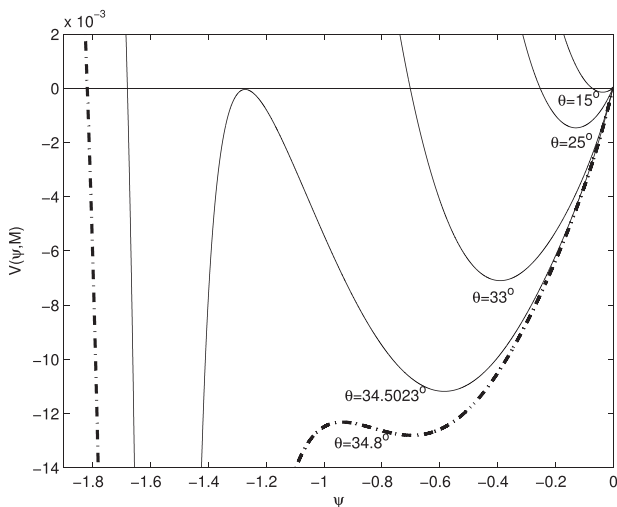
FIG. 9. Sagdeev potential, $V(\psi, M)$, vs. normalized electrostatic potential, ψ, for $f = 0.1$, $M = 0.98$, $\kappa = 10$, and $\tau = 0.04$.
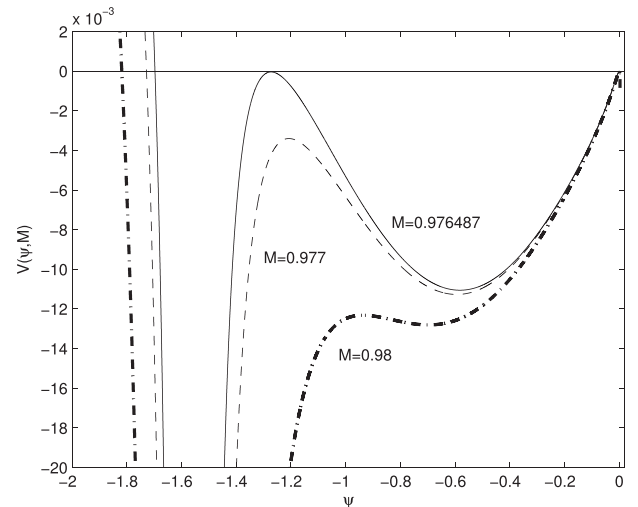
FIG. 11. Sagdeev potential, $V(\psi, M)$, vs. normalized electrostatic potential ψ, for $\theta = 34.8°$, $\kappa = 10$, $f = 0.1$, and $\tau = 0.04$.

TABLE I. Properties of ion-acoustic solitons, such as Soliton Velocity (V), Mach number range ($M_o < M < M_1$), Electric Field (E), Soliton Width (W), and Pulse Duration (τ^*), for various values of the superthermal hot electron (κ) with $\theta = 15°$, normalized cool electron density $f = 0.1$, and cool to hot electron temperature $\tau = 0.04$.

κ	$M_o - M_1$	V (kms^{-1})	E (mV m^{-1})	W (m)	τ^*(ms)
3.0	0.8908–0.920	23.07–23.83	0.01–5.29	1029.6–182.0	44.63–7.64
5.0	0.9320–0.9630	24.14–24.94	0.02–3.79	676.0–174.2	28.00–6.98
10	0.9520–0.9835	24.66–25.47	0.03–3.28	566.8–172.65	22.98–6.78
15	0.9577–0.9900	24.80–25.64	0.04–3.26	530.4–171.6	21.39–6.69
20	0.9604–0.9925	24.87–25.71	0.05–3.20	494.0–171.6	19.86–6.67

applied to the observed parameters in the auroral region, namely, $n_c = 0.2 \, \text{cm}^3$, $n_h = 1.8 \, \text{cm}^3$, $T_c = 1 \, \text{eV}$, and $T_h = 26 \, \text{eV}$, which gives $T_{eff} \approx 7 \, \text{eV}$. The supersoliton electric field amplitude, width, pulse duration, and velocity for $M = 0.98$, $\theta = 34.5023°$, and $\kappa = 10$ come out to be 17.8 mV/m, 663 m, 26.1 ms, and 25.38 km/s, respectively. The present theoretical results agree with the spacecraft measurements.

ACKNOWLEDGMENTS

[1]V. M. Vasyliunas, J. Geophys. Res. **73**, 2839, doi:10.1029/JA073i009p02839 (1968).

[2]M. P. Leubner, J. Geophys. Res. **87**, 6335–6338, doi:10.1029/JA087iA08p06335 (1982).

[3]T. P. Armstrong, M. T. Paonessa, E. V. Bell II, and S. M. Krimigis, J. Geophys. Res. **88**, 8893–8904, doi:10.1029/JA088iA11p08893 (1983).

[4]R. Boström, G. Gustafsson, B. Holback, G. Holmgren, H. Koskinen, and P. Kintner, Phys. Rev. Lett. **61**, 82–85 (1988).

[5]R. Boström, IEEE Trans. Plasma Sci. **20**, 756–0763 (1992).

[6]P. O. Dovner, A. I. Eriksson, R. Boström, and B. Holback, Geophys. Res. Lett. **21**, 1827–1830, doi:10.1029/94GL00886 (1994).

[7]R. A. Cairns, A. A. Mamum, R. Bingham, R. Boström, R. O. Dendy, C. M. C. Nairn, and P. K. Shukla, Geophys. Res. Lett. **22**, 2709–2712, doi:10.1029/95GL02781 (1995).

[8]G. Malka, J. Fuchs, F. Amiranoff, S. D. Baton, R. Gaillard, J. L. Miquel, H. Pepin, C. Rousseaux, G. M. Bonnaud, and L. Lours, Phys. Rev. Lett. **79**, 2053 (1997).

[9]G. Sarri, M. E. Dieckmann, C. R. D. Brown, C. A. Cecchetti, D. J. Hoarty, S. F. James, R. Jung, I. Kourakis, H. Schamel, O. Willi, and M. Borghesi, Phys. Plasmas **17**, 010701 (2010).

[10]A. F. Vinas, H. K. Wong, and A. J. Klimas, Astrophys. J. **528**, 509 (2000).

[11]M. P. Leubner, Sapce Sci. Rev. **107**, 361 (2003).

[12]C. Tsallis, J. Stat. Phys. **52**, 479 (1988).

[13]B. Abraham-Shrauner, J. R. Asbridge, S. J. Bame, and W. C. Feldman, J. Geophys. Res. **84**, 553, doi:10.1029/JA084iA02p00553 (1979).

[14]A. T. Y. Lui and S. M. Krimigis, Geophys. Res. Lett. **8**, 527, doi:10.1029/GL008i005p00527 (1981).

[15]M. R. Collier and D. C. Hamilton, Geophys. Res. Lett. **22**(3), 303–306, doi:10.1029/94GL02997 (1995).

[16]P. Schippers, M. Blanc, N. Andre, I. Dandouras, G. R. Lewis, L. K. Gilbert, A. M. Persoon, N. Krupp, D. A. Gurnett, A. J. Coates, S. M. Krimigis, D. T. Young, and M. K. Dougherty, J. Geophys. Res. **113**, A07208, doi:10.1029/2008JA013098 (2008).

[17]M. Temerin, K. Cerny, W. Lotko, and F. S. Mozer, Phys. Rev. Lett. **48**, 1175 (1982).

[18]R. E. Ergun, C. W. Carlson, J. P. McFadden, F. S. Mozer, G. T. Delory, W. Peria, C. C. Chaston, M. Temerin, I. Roth, L. Muschietti, R. Elphic, R. Strangeway, R. Pfaff, C. A. Cattel, D. Klumpar, E. Shelley, W. Peterson, E. Moebius, and L. Kistler, Geophys. Res. Lett. **25**, 2041, doi:10.1029/98GL00636 (1998).

[19]J. P. McFadden, C. W. Carlson, and R. Ergun, J. Geophys. Res. **104**, 14453–14480, doi:10.1029/1998JA900167 (1999).

[20]C. A. Cattel, J. Crumley, J. Dombeck, R. Lysak, C. Kletzing, W. K. Peterson, and C. Collin, Adv. Space Res. **28**, 1631–1641 (2001).

[21]R. Bharuthram and P. K. Shukla, Phys. Scr. **34**, 732–735 (1985).

[22]R. Bharuthram and P. K. Shukla, Phys. Fluids. **29**, 3214 (1986).

[23]S. Baboolal, R. Bharuthram, and M. A. Hellberg, J. Plasma Phys. **44**, 1 (1990).

[24]R. V. Reddy, G. S. Lakhina, and F. Verheest, Planet Space Sci. **40**(8) 1055–1062 (1992).

[25]L. L. Yadav, R. S. Tiwari, K. P. Maheshwari, and S. R. Sharma, Phys. Rev. E **52**, 3045 (1995).

[26]M. Berthomier, R. Pottelette, and M. Malingre, J. Geophys. Res. **103**(A3) 4261–4270, doi:10.1029/97JA00338 (1998).

[27]S. S. Ghosh and A. N. S. Iyengar, J. Plasma Phys. **67**, 223–233 (2002).

[28]S. S. Ghosh and G. S. Lakhina, Non–lin. Proc. Geophys. **11**, 219–228 (2004).

[29]T. K. Baluku, M. A. Hellberg, and F. Verheest, EPL **91**, 15001 (2010).

[30]T. K. Baluku, M. A. Hellberg, I. Kourakis, and N. S. Saini, Phys. Plasmas **17**, 053702 (2010).

[31]O. R. Rufai, R. Bharuthram, S. V. Singh, and G. S. Lakhina, Phys. Plasmas **19**, 122308 (2012).

[32]O. R. Rufai, R. Bharuthram, S. V. Singh, and G. S. Lakhina, Commun. Nonlinear Sci. Numer. Simul. **19**, 1338–1346 (2014).

[33]N. S. Saini and I. Kourakis, Plasma Phys. Controlled Fusion **52**, 075009 (2010).

[34]S. A. El-Tantawy and W. M. Moslem, Phys. Plasmas **18**, 112105 (2011).

[35]Y.-D. Jung and W.-P. Hong, Phys. Plasmas **18**, 024502 (2011).

[36]S. V. Singh, S. Devanandhan, G. S. Lakhina, and R. Bharuthram, Phys. Plasmas **20**, 012306 (2013).

[37]M. S. Alam, M. M. Masud, and A. A. Mamun, Chin. Phys. B **22**(11), 115202 (2013).

[38]A. E. Dubinov and D. Yu. Kolotkov, IEEE Trans. Plasma Sci. **40**, 1429 (2012).

[39]A. E. Dubinov, Plasma Phys. Rep. **35**, 991–993 (2009).

[40]A. E. Dubinov, Phys. Scr. **80**, 035504 (2009).

[41]A. E. Dubinov, S. K. Saikov, and A. P. Tsatskin, J. Exp. Theor. Phys. **112**, 1051–1060 (2010).

[42]S. K. Maharaj, R. Bharuthram, S. V. Singh, and G. S. Lakhina, Phys. Plasmas **20**, 083705 (2013).

[43]F. Verheest, G. S. Lakhina, and M. A. Hellberg, Phys. Plasmas **21**, 062303 (2014).

[44]G. S. Lakhina, S. V. Singh, and A. P. Kakad, Phys. Plasmas **21**, 062311 (2014).

[45]S. V. Singh and G. S. Lakhina, Commun. Nonlinear Sci. Numer. Simulat. **23**, 274–281 (2015).

[46]F. Verheest, M. A. Hellberg, and I. Kourakis, Phys. Plasmas **20**, 012302 (2013).

[47]F. Verheest, M. A. Hellberg, and I. Kourakis, Phys. Plasmas **20**, 082309 (2013).

[48]F. Verheest, M. A. Hellberg, and I. Kourakis, Phys. Rev. E **87**, 043107 (2013).

[49]O. R. Rufai, R. Bharuthram, S. V. Singh, and G. S. Lakhina, Phys. Plasmas **21**, 082304 (2014).

[50]O. R. Rufai, Phys. Plasmas **22**, 052309 (2015).

[51]S. Sultana, I. Kourakis, N. S. Saini, and M. A. Hellberg, Phys. Plasmas **17**, 032310 (2010).

[52]A. Danehkar, N. S. Saini, M. A. Hellberg, and I. Kourakis, Phys. Plasmas **18**, 072902 (2011).

[53]C. R. Choi, D. Y. Lee, and Y. Kim, J. Astron. Space Sci. **23**(3), 209–216 (2006).